Express Polymer Letters Vol.17, No.7 (2023) 690–698
Available online at www.expresspolymlett.com
https://doi.org/10.3144/expresspolymlett.2023.51

Research article

The effect of crosslink density on the cold crystallization behavior of polybutadiene elastomers

Arpan Datta Sarma[1,2*], *Erathimmanna Bhoje Gowd*[3], *Amit Das*[1], *Gert Heinrich*[1,4]

[1]Leibniz-Institut für Polymerforschung Dresden e.V, D-01069 Dresden, Germany
[2]Luxembourg Institute of Science and Technology, 4362 Esch-sur-Alzette, Luxembourg
[3]Materials Science and Technology Division, CSIR-National Institute for Interdisciplinary Science and Technology, Trivandrum, 695019 Kerala, India
[4]Technische Universität Dresden, 01062 Dresden, Germany

Received 11 December 2022; accepted in revised form 10 February 2023

Abstract. This report presents an insightful investigation of the cold crystallization behavior of sulfur-crosslinked polybutadiene elastomers. The influence of crosslink density on the cold crystallization activities of sulfur-crosslinked polybutadiene rubber (BR) is investigated using differential scanning calorimetry, dynamic mechanical analysis, and X-ray techniques. A significant increase in storage modulus (E') is observed at a temperature just above the glass transition temperature (T_g). This behavior was found to be highly dependent on the crosslink density of the rubber. The dynamic mechanical behavior of the sulfur crosslinked BR is supported by further studies using differential scanning calorimetry and low-temperature X-ray diffraction. This study could contribute to a better understanding of the behavior of BR-containing tire tread rubbers at lower temperatures.

Keywords: *butadiene rubber, cold crystallization, low-temperature modulus, low-temperature X-ray diffraction, dynamic mechanical analysis*

1. Introduction

Crystallization is a process by which molecular building blocks spontaneously organize into an orderly three-dimensional structure to form a solid substance. The crystallization behavior and crystallinity of polymers are different from low-molecular-weight materials [1]. Long-chain polymeric molecules can consist of both a 'crystallizable part' and a 'non-crystallizable part' (amorphous part). The non-crystallizable, amorphous part consists of chain ends, branching points, twisting points, entanglements, and tie molecules [2]. If it is possible to maintain equilibrium throughout the crystallization process and if the initial distribution of the crystallizable-amorphous fraction is known, the equilibrium distribution of crystallites as a function of temperature can be described by Flory's theory [2]. Despite its popularity in polymer physics, the clear and complete concept of the polymer crystallization process has not yet been well established [3–5]. The main reason for this fact is that the process of crystallization depends on both equilibrium (thermodynamically controlled) and non-equilibrium (kinetically controlled) factors which are very complex for polymeric materials [6].

Extensive works have been done to understand the crystallization behavior of semicrystalline polymers. A semicrystalline polymer is capable of crystallizing not only from the molten state (known as melt crystallization) but also from the glassy phase (known as cold crystallization). Limited studies have been reported on the cold crystallization behavior of polymers compared to the melt crystallization behavior.

*Corresponding author, e-mail: arpan.dattasarma@list.lu

Cold crystallization can influence the mechanical properties of the products during their usage in real environments. Above the glass transition temperature, cold crystallization can occur by the formation of folded lamellar morphology and results in semicrystalline morphology at the nanometer level [7]. According to Wunderlich *et al*. [2], this is a random type of crystallization that occurs without any redistribution of molecules but allows only the neighboring amorphous state to crystallize. Due to the high molecular weight and randomness, rubber molecules are generally amorphous [8]. However, a few rubbery materials with high *cis* content show some exceptional behaviors regarding specific orientation and crystallization induced by strain and/or low temperature. Rubbery materials, namely polyisoprene (natural and synthetic), polybutadiene (BR), hydrogenated acrylonitrile butadiene rubber (HNBR), and polychloroprene fall in that category [9–12]. In a recent paper by Schawe *et al*. [13], the structural relaxation of HNBR in the glass temperature range is discussed, where the tetramethylene unit (produced by the hydrogenation of the butadiene unit of the HNBR copolymer) offers the crystalline tendency at glassy region. It is emphasized that a rigid amorphous fraction around the small crystallites limits the further growth of the crystals [13].

It has been reported already that the rate of crystallization of polybutadiene depends on the microstructural purity [14]. Polybutadienes with ~97% *cis* content show an almost ten times faster rate of crystallization than the same material with ~90% cis content [15]. The rate of the crystallization can be denoted as crystallization half-time, the time required for the crystallization of half of the crystallizable segments. The value of crystallization half-time is calculated to be infinite at glass transition temperature and equilibrium melting temperature. In addition, the heating/cooling rate has been identified as a key parameter in controlling the crystallization/cold crystallization behaviors of elastomeric systems [12].

Several techniques have been developed to study the crystallization of semicrystalline polymers. Out of them, differential scanning calorimetry (DSC) [16–18], wide-angle X-ray scattering [7, 19], transmission electron microscopy (TEM) [20], atomic force microscopy (AFM) [21], fluorescence spectroscopy [22], infrared (IR) spectroscopy [16, 23] and vibrational circular dichroism [24] are well-practiced. There are very limited reports regarding the cold crystallization of rubbery materials. Besides, the possibility of using mechanical characterization methods (*e.g.*, dynamic mechanical analysis, DMA) to understand the cold crystallization behaviors has been neglected throughout. The lack of a detailed report on cold crystallization behaviors of rubbery materials and its dependency on the crosslink density of the system have inspired the authors to investigate the current domain.

The main aim of the current topic was to understand the cold crystallization behavior of polybutadiene rubber networks having different crosslink densities. To follow the mentioned aim, butadiene rubber was compounded with different amounts of crosslinking chemicals and vulcanized. The compounds were designed to show different crosslink densities. In order to understand the effect of crosslink density on the cold crystallization behavior of the system, the vulcanized rubber compounds were characterized by DSC, low-temperature X-ray diffraction, and DMA.

2. Experimental

2.1. Materials

Neodymium-catalyzed polybutadiene rubber (Buna CB 24) with 96% cis content and Mooney viscosity of 44 (ML (1+4) at 100 °C) was procured from LANXESS Deutschland GmbH (Köln, Germany). ZnO was procured from ACS reagent, while stearic acid was purchased from Fisher Scientific GmbH (Schwerte, Germany). *N*-cyclohexyl-2-benzothiazole sulfenamide (CBS; Vulkacit CZ/ EG-C) was purchased from Lanxess. Sulfur (S), and toluene (95%) both were purchased from Thermo Fisher Scientific (Geel, Belgium). All the rubber chemicals used for the present study were of technical grade.

2.2. Mixing

All the mixing experiments were carried out in a laboratory-scale two-roll mill (Polymix 110 L, size: 203×102 mm, Servitech GmbH, Wustermark, Germany) at 40 °C. First, the rubber was masticated (~1 min) and a uniform band was produced on the front roll. The nip gap was adjusted (~1 mm) to obtain a suitable bank on top of the mill. ZnO and stearic acid (St. A.) were added and mixed with the rubber for another two minutes. The curatives (CBS and S) were then added to the bank and mixed for further two more minutes until a uniform rubber compound is formed. After complete mixing, the compounded rubber was sheeted out and cooled. The

Table 1. Formulation of a series of polybutadiene compounds formulated with different amounts of curatives; the formulations are given in parts per hundred parts of rubber [phr] unit.

Sample name	Polybutadiene	ZnO	St A	CBS	S
Sample 1	100	3	2	0.75	1
Sample 2	100	3	2	1.50	2
Sample 3	100	3	2	2.25	3

samples were then matured for 3–4 hours and subjected to a rheological analysis using a rotorless vulcameter, Elastograph (Germany), at 150 °C. The optimum cure time was calculated from the respective cure curves obtained from the vulcameter. The optimum cure time was defined by the time required to achieve 90% of the maximum-observed cure torque as obtained from the vulcameter. The rubber compounds were then cured with respect to their cure times using a hot press (Fontijne Holland, Model TP400, Delft, The Netherlands), operating at a temperature of 150 °C temperature and a pressure of 15 MPa. A square shape picture frame mold was used to shape the materials. Depending on the specific gravity of the material and the geometry of the mold an appropriate amount of material was placed inside the mold, resulting in a 1.9–2.1 mm thick rubber sheet. The recipes for all the rubber samples are shown in Table 1. It is worth noting that the ratio between the curing agents (CBS and S) remained the same throughout the formulation of the different rubber compounds.

2.3. Crosslink density

A small piece (0.10±0.02 g) of a square-shaped cured rubber sample was kept in toluene (~20 ml) in a stopped bottle. The solvent was changed after every 24 hours, and the swollen weight of the sample was noted. After the equilibrium swelling was reached (which was confirmed by the same weight of the rubber samples for two consecutive days), the samples were taken out, the excess solvent was wept by blotting paper, and the swollen weight was noted. The sample was then dried (at 60 °C in an oven for 6–8 hours) and weighed again. The crosslink density was estimated by the Flory-Rehner equation [25–27], as described in Equation (1):

$$\nu_e = \frac{-\ln(1-V_r)+V_r+\chi V_r^2}{V_1\left(V_r^{1/3}-\frac{V_r}{2}\right)} = \frac{\rho_p}{M_c} \quad (1)$$

where ν_e is the effective number of chains in a real network/unit volume, V_r is the polymer volume fraction in a swollen network in equilibrium with pure solvent and can be calculated using Equation (2). χ is designated as polymer-solvent interaction parameter and V_1 is the solvent's molar volume. The molecular weight of the polymer segment between two successive crosslinks (M_c) can be expressed as a ratio of the density of the polymer (ρ_p = 0.91 g/cm^3) and the crosslink density of the composite [28]:

$$V_r = \frac{\frac{\text{Weight of dry rubber}}{\text{Density of rubber}}}{\frac{\text{Weight of dry rubber}}{\text{Density of rubber}}+\frac{\text{Weight of absorbed solvent}}{\text{Density of solvent}}} \quad (2)$$

2.4. Differential scanning calorimetry

The cured rubber samples were subjected to a calorimetric study using a differential scanning calorimeter (DSC), Q2000 V24.11 (TA Instruments, USA). The studies were performed with ~10±2 mg of cured samples using standard aluminum pans in an inert atmosphere of nitrogen. The experiments were conducted in a temperature range of –90 to 100 °C with a heating/cooling rate of 3 °C per minute. The samples were first cooled from room temperature to –90 °C, then successive heating, cooling, and heating cycle were performed for all the samples.

2.5. Low-temperature X-ray scattering

Low-temperature X-ray scattering experiments were carried out using a XEUSS X-ray scattering system from Xenocs (operated at 50 kV and 0.60 mA) in transmission geometry using Cu K_α radiation (wavelength, λ = 1.54 Å). The distance between the sample and detector was calibrated using a silver behenate. The scanning was carried out at different temperatures using a hot stage fitted with liquid nitrogen-flowing equipment. The degrees of crystallinity, χ_c, of different samples were calculated using Equation (3) [29]. The size of the crystallites were estimated using the Scherrer equation [30], with a value of the Scherrer constant of 0.9 [31]:

$$\chi_c = \frac{A_c}{A_a + A_c} \quad (3)$$

A_c and A_a are the areas of the crystalline peak and the amorphous signal, respectively, from the deconvoluted X-ray plots.

2.6. Dynamic mechanical analysis

The samples for dynamic mechanical analysis were punched out from the cured rubber sheet with a dimension of 10×5±0.1×2±0.1 cm (L×B×T) using an internally customized die. The samples were then conditioned for 16–20 hours at 23±3 °C before the experiment. Temperature sweep experiments were performed in tensile mode using a dynamic mechanical analyzer GABO EPLEXOR® (Netzsch, Germany) with a 2000 N load cell. The measurements were carried out within the temperature range of –120 to +80 °C with a heating rate of 2 °C/min at a frequency of 10 Hz under 1% static and 0.2% dynamic strain (strain-controlled mode). The samples were first cooled from room temperature to –120 °C, then the experiments were carried out. A soaking time of 60 s was provided to allow the sample to equilibrate with the starting temperature before the start of each cycle.

2.7. Plotting and data interpretation

OriginPro 2019b was used to plot all the results. The inbuild 'Gaussian' function in that software was used to perform the deconvolution of low-temperature X-ray scattering plots. The deconvoluted plots were then used for the calculation of the degree of crystallinity and size of crystallites.

3. Results and discussion

3.1. Crosslink densities of different rubber samples

All the cured rubber samples were subjected to crosslink density measurement via the equilibrium swelling method taking toluene as the solvent (molar volume V_1 = 106.3 cm^3/mol). The value of the polymer-solvent interaction parameter (χ = 0.34) was used in the calculation as referred in previous reports [32, 33]. The values of the estimated crosslink densities and the values of the molecular weights between the successive crosslinks of all the samples are collected and tabulated in Table 2. From Table 2, a change in the order of magnitude of crosslink densities can be observed. As expected, the values of crosslink densities of the samples are proportional to the content of curatives in the formulation.

3.2. Differential scanning calorimetric analysis of different cured rubber samples

The cooling and the second heating curves as obtained from DSC measurements are shown in Figure 1, where the cooling cycles are denoted by dotted lines, and the heating cycles are denoted by solid ones. During the cooling cycle, exothermic peaks (around –60 to –45 °C) associated with melt crystallization were observed for Samples 1 and 2. Sample 1 showed a sharp crystallization peak (FWHM = 11.3), while the crystallization peak for Sample 2 was found to be broad (FWHM = 17.9). The sharpness of the exothermic peak may indicate the homogeneity of the crystal structure. During the second heating cycle, exothermic peaks associated with cold crystallization were observed (around –66 to –55 °C) for Samples 2 and 3. The width of the cold crystallization peak for Sample 2 and Sample 3 were found to be comparable (FWHM for Sample 2 = 11.3 *vs.* Sample 3 = 11.6). The exothermic peak of cold crystallization was found to be followed by an endothermic peak (around –30 to –15 °C) for all the samples,

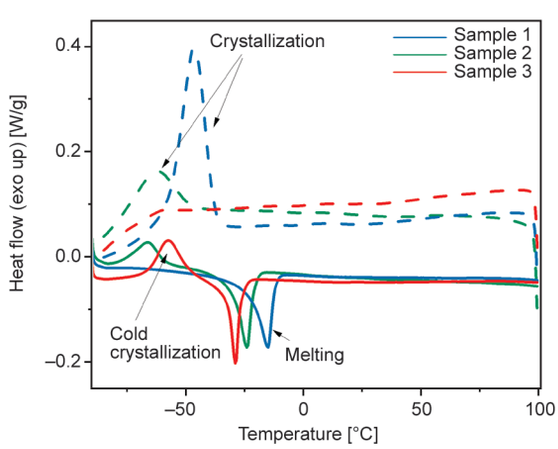

Figure 1. Cooling and second heating cycles of polybutadiene rubber samples with different crosslink densities as obtained from DSC studies. The cooling curves are shown by the dotted lines where the heating curves are designated by solid lines.

Table 2. Crosslink densities of cured polybutadiene samples containing different amounts of curatives.

Sample name	Crosslink density [mol/cm^3]	Average molecular weight between two successive crosslinks [g/mol]
Sample 1	$8.8\cdot10^{-5}\pm2\cdot10^{-6}$	10 300±350
Sample 2	$19.0\cdot10^{-5}\pm1\cdot10^{-6}$	4 800±48
Sample 3	$22.6\cdot10^{-5}\pm1\cdot10^{-6}$	4 000±30

which might denote the melting of the crystals. Associating the exothermic peak intensities with the percentage of crystallinity, a decreasing tendency of the percentage of crystallinity was observed from the figure as a function of crosslink density. It can be argued that due to the increased crosslink density, it was difficult for the rubber chains to organize themselves to attain regular structures. The argument can be supported by the almost negligible peak intensity of crystallization for Sample 3 during the cooling cycle. On the other hand, with the lowest crosslink density, it was most favorable for the molecules of Sample 1 to form the crystalline domains, which was reflected by the highest exothermic peak intensity during the cooling cycle.

Due to the constraints imposed by the crosslinked structure, the molecules of the highly crosslinked samples (Sample 2 and Sample 3) were unable to align during the cooling cycle. Because of this inability, the molecules tend to orient themselves during the heating cycle. It is possible that due to the low degree of crosslinking, the molecules of Sample 1 crystallized during cooling and no cold crystallization was observed during the heating cycle. The molecular mobility caused by the thermal energy has contributed to the more crosslinked molecules arranging themselves in regular order and achieving a kind of crystallinity. This phenomenon can be related to cold crystallization. As the process is kinetically limited for Sample 3, the cold crystallization peak appears at a higher temperature for this sample. It should also be noted that a higher chance of crystallization during the cooling cycle is associated with a lower chance of cold crystallization during the heating cycle.

This statement can be supported by the values of enthalpies tabulated in Table 3, where it is shown that the sum of the enthalpy of melt crystallization (ΔH_{cry}) and the enthalpy of cold crystallization (ΔH_{cold}) is equal to the melting enthalpy (ΔH_{melt}). The melting enthalpy can be regarded as a measure of the overall percentage of crystallinity. With the lowest crosslink density, Sample 1 shows the highest percentage of crystallinity as shown in Table 3.

3.3. Low-temperature X-ray diffraction studies of different cured rubber samples

Low-temperature X-ray diffraction studies were conducted to understand the effect of crosslink density on the cold crystallization behavior of polybutadiene elastomer. The study was conducted within the temperature range of –100 and 20 °C. The diffraction patterns were recorded at a regular interval of 20 °C while heating the melt-cooled samples and are reported in Figure 2. Two distinct peaks corresponding to the crystalline domains of the crosslinked polybutadiene elastomer at 2θ of 19° and 22.7° can be seen in the diffraction patterns of the individual samples, which is consistent with the previous report [33]. The peak at 2θ of 19° corresponds to the crystal plane of (020), while the other one (22.7°) corresponds to the (110) plane. Among the studied samples, Sample 1 was found to be the most crystalline, while the percentage of crystallinity was observed to decrease as a function of the crosslink density of the elastomeric samples. As observed in DSC thermograms, the melt-cooled samples crystallized upon cooling, and no cold crystallization was observed during heating in the case of Sample 1. It was found that the peaks corresponding to the crystalline domains of Sample 1 decrease with increasing temperature and disappear beyond the temperature of 0 °C. The disappearance of the characteristic peaks may correspond to the melting of the crystalline domains of Sample 1. Sample 3, on the other hand, was found to show no crystalline peaks at the beginning; however, the characteristic peaks of crystalline polybutadiene domains appeared upon heating. The two distinct peaks at 2θ of 19.0 and 22.7° were clearly observed when the temperature was raised to –60 °C (from –80 °C). The appearance of the mentioned peaks may correspond to the cold crystallization of

Table 3. Enthalpy values for crystallization, cold crystallization, and melting for the crystalline domains, along with the respective transition temperatures for a series of cured rubber samples of different crosslink densities.

Sample name	Enthalpy of crystallization (during the cooling cycle), ΔH_{cry} [J/g]	Enthalpy of cold crystallization, ΔH_{cold} [J/g]	T_{melt} [°C]	T_{cryst} [°C]	$T_{coldcryst}$ [°C]	$\Delta H_{cry} + \Delta H_{cold}$ [J/g]	Melting enthalpy, ΔH_{melt} [J/g]
Sample 1	29.02	0.38	–31	–32	–68	29.40	26.03
Sample 2	13.54	8.50	–36	–44	–78	22.04	22.53
Sample 3	0	16.80	–40	N.A.	–70	16.80	17.65

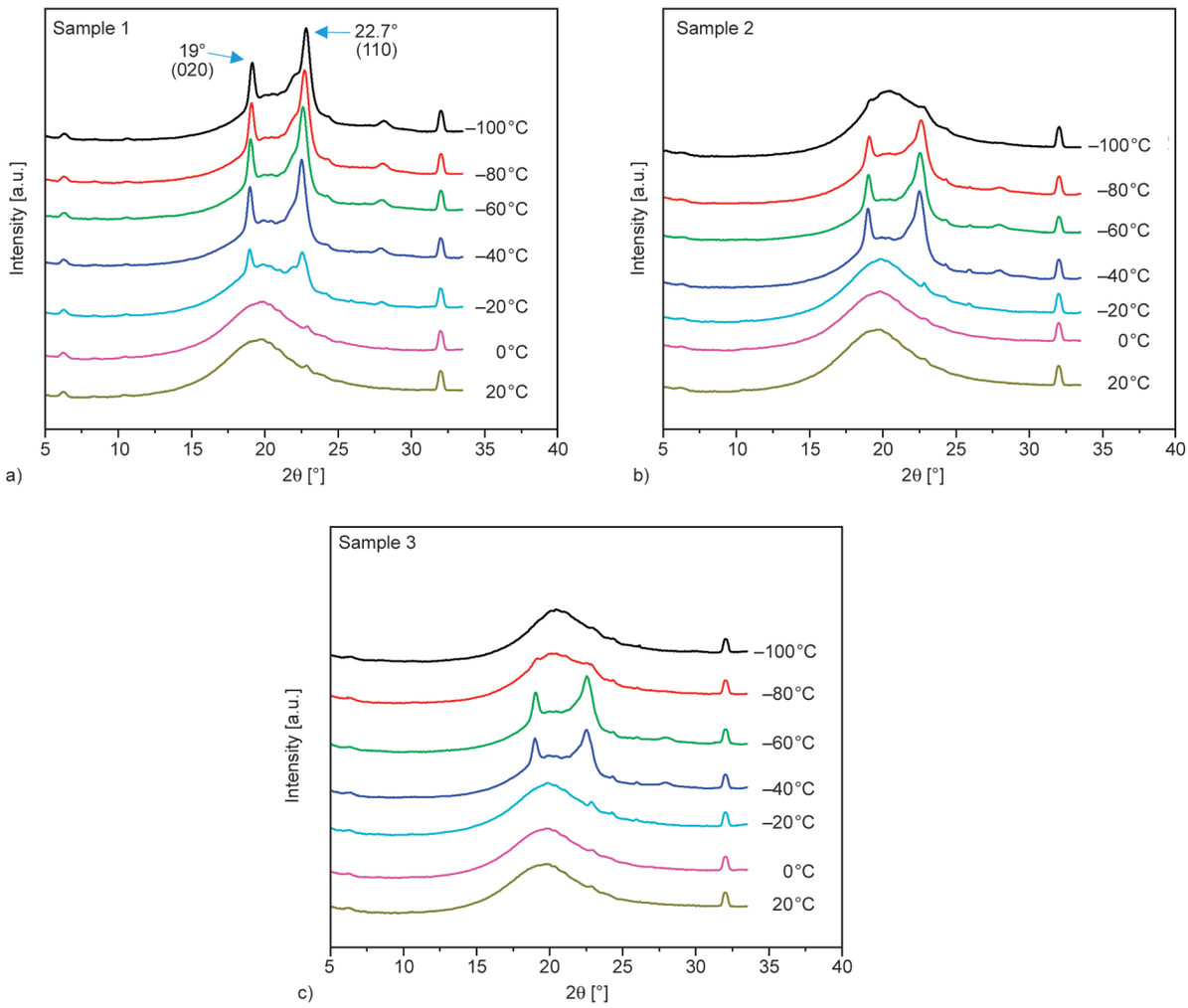

Figure 2. Low-temperature X-ray analysis of a series of cured polybutadiene rubber samples with different crosslink densities, showing different cold crystallization behaviors: a) Sample 1, b) Sample 2, c) Sample 3.

the crosslinked polybutadiene elastomer. The crystalline peaks were found to disappear beyond –20 °C for Sample 3. These observations are in good agreement with the DSC data. The cold crystallization behavior was also observed for Sample 2; the crystalline peaks appeared upon heating (at –80 °C) and disappeared beyond –20 °C. The order of disappearance of the crystalline peaks follows the same trend of melting endotherms as observed during the DSC analysis, Sample 3 the first and Sample 1 at a higher temperature. As discussed previously, the higher the crosslink density, the higher the chance of cold crystallization for elastomeric samples, which can be observed during low-temperature X-ray diffraction studies. At the same time, with the highest crosslink density, Sample 3 was found to require a higher amount of thermal energy to orient the polymer segments, which is in line with the previous observations.

The low-temperature X-ray plots were further deconvoluted to isolate the crystalline peaks and the amorphous signal. As an example, the deconvoluted plot of Sample 2 at –60 °C is shown in Figure 3. The full width at half maxima (FWHM) and area of the deconvoluted plots were extracted from each deconvoluted X-ray image and used to calculate degree of crystallinity (χ_c) and the size of crystallites. The Scherrer equation was used to estimate the size of the crystalline domains. The estimated results are gathered and shown in Table 4. From Table 4, the largest crystallite sizes can be observed for Sample 1 (~18 nm crystals with (020) plane and ~11–12 nm crystals with (110) plane), while the smallest crystallite sizes were observed for Sample 3 (~15 nm crystals with (020) plane and ~8–9 nm crystals with (110) plane). The largest size of the crystalline domain can support the DSC observation of the highest melting temperature along with the broadest melting

Table 4. Degree of crystallinity and size of the crystalline domains for a series of cured rubber samples of different crosslink densities.

Temperature [°C]	Sample 1			Sample 2			Sample 3		
	χ_c	Crystal size (020) [nm]	Crystal size (110) [nm]	χ_c	Crystal size (020) [nm]	Crystal size (110) [nm]	χ_c	Crystal size (020) [nm]	Crystal size (110) [nm]
–100	0.27	18.52	13.32	0	N.A.	N.A.	0	N.A.	N.A.
–80	0.28	18.10	12.88	0.19	14.74	9.70	0	N.A.	N.A.
–60	0.29	17.69	12.47	0.26	15.61	9.47	0.26	14.74	8.83
–40	0.25	18.96	10.62	0.24	16.25	9.47	0.22	15.31	9.14
–20	0.11	18.10	11.39	0	N.A.	N.A.	0	N.A.	N.A.
0	0	N.A.	N.A.	0	N.A.	N.A.	0	N.A.	N.A.
20	0	N.A.	N.A.	0	N.A.	N.A.	0	N.A.	N.A.

endotherm for Sample 1. A linear proportionality can be observed for the crystal size and the melting temperature as observed by DSC. The degree of crystallinity for all the samples, regardless of the crosslink density, was found to be maximum at –60 °C. This can be due to the cumulative effect of the crystallinity and cold crystallinity of the sample at this temperature. For Sample 1, the degree of crystallinity was found to decrease above a specific temperature (–40 °C) and disappeared after 0 °C. On the contrary, for other samples, the degree of crystallinity increased upon heating due to cold crystallization, and disappeared after –40 °C. The results are in line with the observations of the DSC analysis.

3.4. Dynamic mechanical analysis of different cure rubber samples

All samples with different crosslink densities were subjected to dynamic mechanical analysis (DMA). The experiments were carried out in a strain-controlled mode of DMA [9]. The temperature response diagrams are shown in Figure 4. A glass-rubber transition for the crosslinked rubber samples can be observed at about –90 °C. With the highest percentage of crystallinity, Sample 1 showed a minimal decrease in storage modulus during the glass-rubber transition, while Sample 3 showed the largest decrease. The decrease in storage modulus was then followed by an increase in storage modulus for Samples 2 and 3 (at –70 to –60 °C). This unusual increase in storage modulus after the glass transition temperature may be associated with the formation of crystalline domains during the process of cold crystallization. With the highest number of crosslinks, Sample 3 shows the highest degree of cold crystallization, as previously observed (DSC and low-temperature X-ray studies). Followed by the increase of the modulus for Sample 2 and 3, another drop of

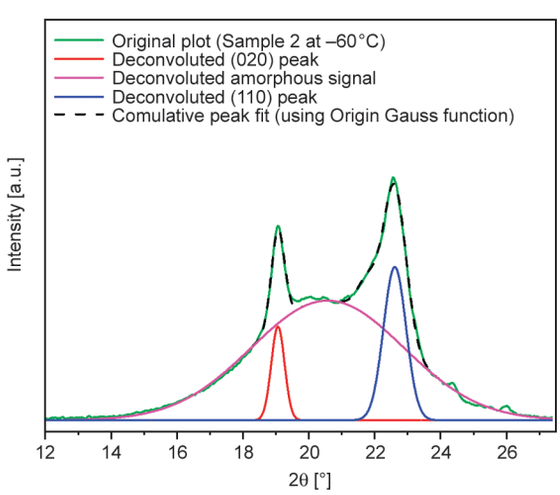

Figure 3. Deconvoluted peaks and cumulative peak fit for Sample 2 at –60 °C as an example for a series of polybutadiene rubber samples with different crosslink densities.

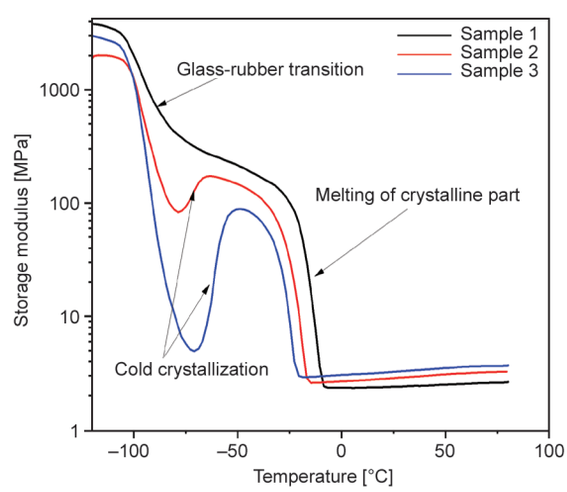

Figure 4. Dynamic mechanical analysis of a series of cured polybutadiene rubber samples with different crosslink densities, showing different cold crystallization behaviors during the glass-rubber transition.

storage modulus (at –27 to –15 °C) was observed for all the samples. The second drop can be associated with the melting of the crystalline domains. It is worth noting that the sample with the lowest crosslink density showed the highest modulus at low temperatures (<–10 °C). Crystallinity may be the leading factor behind the high modulus of the low crosslinked samples at low temperatures. The order of storage modulus of the samples was found to be reversed at a higher temperature. The highest modulus was found for the sample with the highest crosslink density at room temperature, as expected.

4. Conclusions

Polybutadiene rubber with high cis content was compounded with sulfur crosslinking agents to form rubber composites with different crosslink densities. The samples were then subjected to DSC, low-temperature X-ray diffraction, and DMA analysis. In the studies, a characteristic and interesting behavior during cold crystallization, influenced by the crosslink density, was observed. The rubber compound with the lowest crosslink density showed the highest amount of crystallinity and the lowest degree of cold crystallizability, and vice versa. The sudden increase in stiffness of highly crosslinked rubber samples when heated from sub-ambient temperatures to room temperature can be attributed to the cold crystallization of the BR chains. In addition, the samples with low crosslink density were found to have a high modulus below –10 °C, as an effect of a sufficient number of crystalline domains but a low modulus at room temperature. The incorporation of reinforcing fillers and the introduction of different curing systems (peroxide, different S-curing systems with different S to accelerator ratio) may alter the cold crystallization behavior of polybutadiene. A separate study can be envisaged to understand all these effects.

Acknowledgements

We thank Mrs. Sabine Krause (IPF Dresden, Germany) and Mr. Amal Raj for carrying out the DSC and X-ray measurements. G. H. thanks for the German DFG project 380321452/GRK2430.

Experimental works were mainly carried out in IPF Dresden, the authors are thankful to the institution for the facilities and infrastructure

References

[1] Gedde U. W., Hedenqvist M. S.: Crystallization kinetics. in 'Fundamental polymer science' (eds.: Gedde U. W., Hedenqvist M. S.) Springer, Heidelberg, 327–386 (2019). https://doi.org/10.1007/978-3-030-29794-7_8

[2] Wunderlich B.: Theory of cold crystallization of high polymers. The Journal of Chemical Physics, **29**, 1395–1404 (1958). https://doi.org/10.1063/1.1744729

[3] Reiter G., Sommer J-U.: Polymer crystallization: Observations, concepts and interpretations. Springer, Heidelberg (2003). https://doi.org/10.1007/3-540-45851-4

[4] Allegra G., Meille S. V.: Pre-crystalline, high-entropy aggregates: A role in polymer crystallization? in 'Interphases and mesophases in polymer crystallization III' (ed.: Allegra G.) Springer, Heidelberg, 87–135 (2005). https://doi.org/10.1007/12_009

[5] Strobl G.: Crystallization and melting of bulk polymers: New observations, conclusions and a thermodynamic scheme. Progress in Polymer Science, **31**, 398–442 (2006). https://doi.org/10.1016/j.progpolymsci.2006.01.001

[6] Lund R., Alegría A., Goitandía L., Colmenero J., González M. A., Lindner P.: Dynamical and structural aspects of the cold crystallization of poly(dimethylsiloxane) (PDMS). Macromolecules, **41**, 1364–1376 (2008). https://doi.org/10.1021/ma702055b

[7] Šics I., Ezquerra T. A., Nogales A., Denchev Z., Alvarez C., Funari S. S.: Cold crystallization of poly(ethylene naphthalene-2,6-dicarboxylate) by simultaneous measurements of X-ray scattering and dielectric spectroscopy. Polymer (Guildf), **44**, 1045–1049 (2003). https://doi.org/10.1016/S0032-3861(02)00742-5

[8] Gent A. N.: Rubber elasticity: Basic concepts and behavior. in 'The science and technology of rubber' (eds.: Mark J. E., Erman B., Roland C. M.) Academic Press, Boston, 1–26 (2013). https://doi.org/10.1016/B978-0-12-394584-6.00001-7

[9] Wunde M., Klüppel M.: Effect of filler and blending with SBR and NR on thermally induced crystallization of high-cis BR as evaluated by dynamic mechanical analysis. Express Polymer Letters, **14**, 261–271 (2020). https://doi.org/10.3144/expresspolymlett.2020.22

[10] Bukhina K.: Crystallization of elastomers at low temperatures. in 'Low-temperature behaviour of elastomers' (ed.: Bukhina K.) CRC Press, Boca Raton, 59–94 (2007). https://doi.org/10.1201/b12239

[11] Chenal J. M., Chazeau L., Bomal Y., Gauthier C.: New insights into the cold crystallization of filled natural rubber. Journal of Polymer Science Part B: Polymer Physics, **45**, 955–962 (2007). https://doi.org/10.1002/polb.21105

[12] Bertini F., Canetti M., Ricci G.: Crystallization and melting behavior of 1,2-syndiotactic polybutadiene. Journal of Applied Polymer Science, **92**, 1680–1687 (2004). https://doi.org/10.1002/app.20115

[13] Schawe J. E. K., Wrana C.: Competition between structural relaxation and crystallization in the glass transition range of random copolymers. Polymers (Basel), **12**, 1778 (2020). https://doi.org/10.3390/polym12081778

[14] Bruzzone M., Sorta E.: Elastomer structures and 'cold crystallization'. Rubber Chemistry and Technology, **52**, 207–212 (1979). https://doi.org/10.5254/1.3535204

[15] Bekkedahl N., Wood L. A.: Crystallization of vulcanized rubber. Rubber Chemistry and Technology, **14**, 347–355 (1941). https://doi.org/10.5254/1.3540030

[16] Vasanthan N., Manne N. J., Krishnama A.: Effect of molecular orientation on the cold crystallization of amorphous–crystallizable polymers: The case of poly(trimethylene terephthalate). Industrial & Engineering Chemistry Research, **52**, 17920–17926 (2013). https://doi.org/10.1021/ie402860t

[17] Supaphol P., Apiwanthanakorn N.: Nonisothermal cold-crystallization kinetics of poly(trimethylene terephthalate). Journal of Polymer Science Part B: Polymer Physics, **42**, 4151–4163 (2004). https://doi.org/10.1002/polb.20276

[18] Apiwanthanakorn N., Supaphol P., Nithitanakul M.: Non-isothermal melt-crystallization kinetics of poly(trimethylene terephthalate). Polymer Testing, **23**, 817–826 (2004). https://doi.org/10.1016/j.polymertesting.2004.03.001

[19] Mano J. F., Wang Y., Viana J. C., Denchev Z., Oliveira M. J.: Cold crystallization of PLLA studied by simultaneous SAXS and WAXS. Macromolecular Materials and Engineering, **289**, 910–915 (2004). https://doi.org/10.1002/mame.200400097

[20] Ivanov D. A., Pop T., Yoon D. Y., Jonas A. M.: Direct observation of crystal–amorphous interphase in lamellar semicrystalline poly(ethylene terephthalate). Macromolecules, **35**, 9813–9818 (2002). https://doi.org/10.1021/ma011784j

[21] Ivanov D. A., Amalou Z., Magonov S. N.: Real-time evolution of the lamellar organization of poly(ethylene terephthalate) during crystallization from the melt: High-temperature atomic force microscopy study. Macromolecules, **34**, 8944–8952 (2001). https://doi.org/10.1021/ma010809b

[22] Luo W-A., Liao Z., Yan J., Li Y., Chen X., Mai K., Zhang M.: Cold-crystallization of poly(trimethylene terephthalate) studied by photoluminescence of its amorphous portion. Macromolecules, **41**, 7513–7518 (2008). https://doi.org/10.1021/ma801119n

[23] Yoshii T., Yoshida H., Kawai T.: Effect of structural relaxation of glassy PET on crystallization process observed by the simultaneous DSC–XRD and DSC–FTIR. Thermochimica Acta, **431**, 177–181 (2005). https://doi.org/10.1016/j.tca.2005.01.070

[24] Chao Y-K., Praveena N. M., Yang K-C., Gowd E. B., Ho R-M.: Crystallization of polylactides examined by vibrational circular dichroism of intra- and inter-chain chiral interactions. Soft Matter, **18**, 2722–2725 (2022). https://doi.org/10.1039/D2SM00060A

[25] Rooj S., Das A., Thakur V., Mahaling R. N., Bhowmick A. K., Heinrich G.: Preparation and properties of natural nanocomposites based on natural rubber and naturally occurring halloysite nanotubes. Materials & Design, **31**, 2151–2156 (2010). https://doi.org/10.1016/j.matdes.2009.11.009

[26] Flory P. J., Rehner J.: Statistical mechanics of cross-linked polymer networks I. Rubberlike elasticity. The Journal of Chemical Physics, **11**, 512–520 (1943). https://doi.org/10.1063/1.1723791

[27] Vijayabaskar V., Stephan M., Kalaivani S., Volke S., Heinrich G., Dorschner H., Bhowmick A. K., Wagenknecht U.: Influence of radiation temperature on the crosslinking of nitrile rubber by electron beam irradiation. Radiation Physics and Chemistry, **77**, 511–521 (2008). https://doi.org/10.1016/j.radphyschem.2007.09.011

[28] Hoti G., Caldera F., Cecone C., Pedrazzo A. R., Anceschi A., Appleton S. L., Monfared Y. K., Trotta F.: Effect of the cross-linking density on the swelling and rheological behavior of ester-bridged β-cyclodextrin nanosponges. Materials (Basel), **14**, 1–20 (2021). https://doi.org/10.3390/ma14030478

[29] Aziz S. B., Abdullah O. G., Rasheed M. A., Ahmed H. M.: Effect of high salt concentration (HSC) on structural, morphological, and electrical characteristics of chitosan based solid polymer electrolytes. Polymers, **9**, 187 (2017). https://doi.org/10.3390/polym9060187

[30] Kurajica S., Mužina K., Keser S., Dražić G., Munda I. K.: Assessment of cell toxicity and oxidation catalytic activity of nanosized zinc-doped ceria UV filter. Chemical and Biochemical Engineering Quarterly, **35**, 157–164 (2021). https://doi.org/10.15255/CABEQ.2020.1905

[31] Vinila V. S., Isac J.: Synthesis and structural studies of superconducting perovskite $GdBa_2Ca_3Cu_4O_{10.5+\delta}$ nanosystems. in 'Design, fabrication, and characterization of multifunctional nanomaterials' (eds.: Thomas S., Kalarikkal N., Abraham A. R.) Elsevier, Amsterdam, 319–341 (2022). https://doi.org/10.1016/B978-0-12-820558-7.00022-4

[32] Hergenrother W. L.: Characterization of networks from the peroxide cure of polybutadiene. Journal of Applied Polymer Science, **16**, 2611–2622 (1972). https://doi.org/10.1002/app.1972.070161014

[33] Parker W. O., Ferrando A., Ferri D., Canepari V.: Cross-link density of a dispersed rubber measured by ^{129}Xe chemical shift. Macromolecules, **40**, 5787–5790 (2007). https://doi.org/10.1021/ma070793a